l_2 and l_1 Beamformers: Recursive Implementation and Performance Analysis

Victor A. N. Barroso, *Member, IEEE,* and José M. F. Moura, *Fellow, IEEE*

Abstract— **In this paper, we study array beamformers as optimal waveform estimators. We apply an inverse problem formulation, presenting an integrated design to quadratic (l_2) and least absolute value (l_1) beamformers. The general solution of the l_2 beamformers is parameterized by a regularizing parameter that weights the confidence placed by the designer on prior knowledge versus the quality of the measurements. This regularizing parameter is used to establish an equivalence between alternative l_2 beamformers. We then develop time-recursive implementations of the l_2 and l_1 beamformers. The performance of these beamformers is studied next. We show that 1) in the presence of correlated arrivals, the MMSE beamformer uses constructively the correlation between incoming signals in reconstructing the estimated field, while rejecting the uncorrelated returns, and 2) the l_1 beamformer has the ability to adjust itself to unexpected noise conditions because it is considerably more robust than the l_2 beamformers to unmodeled impulsive noise or to the occurrence of malfunctioning sensors. The analysis is confirmed by simulated studies.**

I. Introduction

BEAMFORMERS provide spectral estimates of signals with temporal and spatial contents, e.g., directional propagating fields. The minimum noise power and the minimum variance distortionless signal response (MNPDR, MVDR) beamformers [7], [9] are examples of such well-known optimum quadratic (l_2 norm) receivers. In this paper, we are concerned with the integrated design and the study of the performance of beamformers considered as array processors yielding optimal waveform reconstruction. We adopt an inverse type approach [22]. This inverse problem approach captures several alternative beamformers in an integrated formulation [3]. We study in detail l_2 and l_1 beamformers.

The beamformers' structure is parameterized by a regularizing parameter α. For the l_2 beamformer, we show how specific choices of α, combined with the assumed noise statistics, lead to alternative beamformers like the minimum mean square error (MMSE) [4], the MNPDR, the MVDR, or the conventional delay-and-sum (DS) beamformers.

We present recursive implementations for the l_2 and l_1 beamformers that are based on the Kalman–Bucy filtering theory [15], [16].

Manuscript received November 23, 1990; revised August 2, 1993. The associate editor coordinating the review of this paper and approving it for publication was Prof. S. Unnikrishna Pillai.

V. A. N. Barroso is with CAPS, Department of Electrical and Computer Engineering, Instituto Superior Técnico, Lisbon, Portugal.

J. M. F. Moura is with the Department of Electrical and Computer Engineering, Carnegie Mellon University, Pittsburgh, PA 15213, USA.

IEEE Log Number 9400389.

We turn then to the beamformers' performance study, addressing two situations of practical interest. The first is when there are correlated arrivals. The MMSE beamformer combines coherently all the correlated replicas of the desired signal. This behavior is quite different from that exhibited by the MVDR beamformer, where correlated arrivals are known to cause signal cancellation. In this case, the MNPDR beamformer nulls the correlated arrivals as if they were undesired noisy interferences, whereas the DS beamformer acts like a conventional filter designed on the spatial frequency (wavenumber) domain. The superior performance of the MMSE beamformer for coherent signals is due to the use of prior knowledge of the desired signal. Although this may be a problem in some applications, there are other situations where prior knowledge is available. Underwater robotics, particularly autonomous vehicles technology, is an important emerging field of research and development. Clearly, a true autonomous behavior requires an acoustic communication link between the vehicle and the base station [2]. In addition, it is necessary for the base station to locate and to track the vehicle's trajectory. In both cases, the receiver has knowledge of the signal power spectrum, thus enabling the use of the MMSE beamformer in order to take advantage of the multipath propagation. The second situation of interest is when the actual noise conditions depart significantly from the model assumed for the noise. Although both l_2 and l_1 beamformers exhibit comparable behavior when the observed noise follows the prior assumed statistics, in the presence of unmodeled noise conditions, they have quite distinct performances. This results from the adjustable features of l_1 processors [5], [11], [17], [24], [26]. Contrary to what happens with l_2 processors, which consider all the noise samples as representative of the assumed statistics, l_1 processors adjust themselves to unexpected (less probable) noise samples. We study the case of unexpected impulsive noise with a power level that is much stronger than that of the background noise. We prove that the output error power of the l_2 beamformer is essentially determined by the power of the impulsive noise. On the contrary, the l_1 structure adjusts itself to the observed noise conditions providing signal estimates where the input noise impulses are strongly attenuated. Simulation studies confirm the analytical results derived.

The paper is organized as follows. In Section II, we introduce beamforming as an inverse problem. We consider inversion strategies based on l_2 and l_1 norms. For the l_2 norm, we derive the MMSE beamformer and show how other known beamformers are captured by this integrated design. In the l_1

case, we show how the beamformer gains are adjusted by the level of the residues at the output of the beamformer. Section III develops recursive implementations for both l_1 and l_2 beamformers. Performance studies are carried out in Section IV, particularly for scenarios where correlated arrivals or outliers are present. Simulation results are reported in Section V. Finally, Section VI lists the main conclusions of the paper.

II. Beamforming as an Inverse Problem

The inverse approach is frequently used to solve reconstruction problems in situations where the involved signals are not measured directly. In this section, we address beamforming as an inverse problem.

A. Problem Formulation

In beamforming, the goal is to estimate waveforms arriving from known directions, given a set of noisy measurements collected by an array of N sensors. We restrict our attention to the narrowband beamforming problem. Let

$$z(k) = a(\theta)x(k) + w(k) \tag{2.1}$$

be the complex envelope of the $(N \times 1)$ vector of observations at time k, where $x(\cdot)$ and $w(\cdot)$ are the complex envelopes of the desired signal and of the noise, respectively. The problem is to find the best estimate of $x(\cdot)$ in the sense of minimizing the generic cost functional

$$J = d_1\left(z(k) - a(\theta)x(k); R_w^{-1}\right) + \alpha d_2\left(x(k); R_x^{-1}\right) \tag{2.2}$$

where $d_1(\cdot; R_w^{-1})$ represents a suitable norm defined using the metric R_w^{-1} and similarly for $d_2(\cdot; R_x^{-1})$. In general, the positive definite metrics on which the norms d_1 and d_2 are defined are arbitrary. In this paper, we adopt a statistical context, R_w and R_x being interpreted as noise and signal covariances, respectively. The first term in (2.2) constrains the residues, whereas the second constrains the solution. The regularizing parameter α adjusts the confidence of the designer on the prior knowledge about $x(\cdot)$ versus reliance on the observations. For $\alpha = 0$, total confidence is placed on the measurements. This corresponds to situations where no prior knowledge about the desired signal is available. For $\alpha \neq 0$, $d_1(\cdot;\cdot)$ penalizes the cost associated with the noise model, whereas $d_2(\cdot;\cdot)$ has a smoothing effect on the solution, forcing it to follow the assumed prior signal model.

The norms that we consider are l_p norms of N-dimensional vectors s in the metric of the positive definite matrix R_s. These norms result from the generalization of the usual quadratic norm $s^H R_s^{-1} s$ ($(\cdot)^H$ denotes transpose conjugate) defined for non-Euclidean spaces with metric R_s. For $1 \leq p < \infty$, we define these norms to be

$$l_p(s; R_s^{-1}) = \left[\sum_{n=1}^{N} \left(\frac{|v_n^H s|}{\sqrt{\lambda_n}}\right)^p\right]^{\frac{1}{p}} \tag{2.3}$$

where $\{\lambda_n\}_{n=1}^N$ are the eigenvalues associated with the normalized eigenvectors $\{v_n\}_{n=1}^N$ of R_s. It is easy to verify that (2.3) satisfies all the axioms of a norm. Notice that for $R_s = I$, the general definition (2.3) becomes the usual l_p norm

$$l_p(s) = \left[\sum_{n=1}^{N} |s_n|^p\right]^{\frac{1}{p}} \tag{2.4}$$

where s_n denotes the nth element of vector s. Let $\mathcal{S}$ be the space of vectors s spanned by the orthonormal basis $\{v_n\}_{n=1}^N$. Then, (2.3) weights the contributions of the components of s along each direction v_n by the inverse of the standard deviation $\sqrt{\lambda_n}$.

B. Quadratic Beamforming: $p = 2$

Using quadratic norms $p = 2$, the cost functional (2.2) takes the form

$$J_{l_2} = [z(k) - a(\theta)x(k)]^H R_w^{-1}[z(k) - a(\theta)x(k)] + \alpha x^H(k) R_x^{-1} x(k) \tag{2.5}$$

where R_w and R_x are the noise and the signal covariance matrices, respectively. The minimum of (2.5) is achieved by

$$\hat{x}(k) = \left[\alpha R_x^{-1} + a^H(\theta) R_w^{-1} a(\theta)\right]^{-1} a^H(\theta) R_w^{-1} z(k). \tag{2.6}$$

This is the general solution for the l_2 beamforming problem. Cases of interest are $\alpha = 0$ or $\alpha = 1$. In the following paragraphs, we consider instances of interest of this general result.

1) MMSE Beamformer: Assume that 1) $\alpha = 1$, i.e., prior knowledge and measurements are balanced in the cost functional (2.5), and 2) signal and noise are statistically independent. Equation (2.6) takes the form

$$\hat{x}^{\text{MMSE}}(k) = R_{xz} R_z^{-1} z(k) = \left[R_x^{-1} + a^H(\theta) R_w^{-1} a(\theta)\right]^{-1} a^H(\theta) R_w^{-1} z(k) \tag{2.7}$$

where

$$R_z = a(\theta) R_x a^H(\theta) + R_w \tag{2.8}$$

is the spatial covariance matrix of the observations and

$$R_{xz} = R_x a^H(\theta) \tag{2.9}$$

is the cross-covariance between the signal and the observations. The l_2 beamformer (2.7) is the MMSE solution provided by the optimum Wiener filter [23]. Notice that with $\alpha = 1$, minimizing (2.5) is equivalent to computing the maximum *a posteriori* (MAP) signal estimate for the *Gaussian signal* in *Gaussian noise* problem.

2) MNPDR and MVDR Beamformers: With $\alpha = 0$, absolute confidence is placed on the measurements. Equation (2.6) yields

$$\hat{x}^{\text{MNPDR}}(k) = \frac{a^H(\theta) R_w^{-1}}{a^H(\theta) R_w^{-1} a(\theta)} z(k). \tag{2.10}$$

This formula specifies the MNPDR beamformer and gives the maximum likelihood (ML) signal estimate for the *unknown signal* in the *Gaussian noise* problem. It is known that when signal and noise are statistically independent, the MNPDR and

MVDR beamformers are equivalent [6], and (2.10) can be written as

$$\hat{x}^{\mathrm{MVDR}}(k) = \frac{a^H(\theta)R_z^{-1}}{a^H(\theta)R_z^{-1}a(\theta)}z(k) \tag{2.11}$$

where the noise covariance matrix R_w is replaced by the observations covariance matrix R_z.

3) Conventional Beamformer: If no prior knowledge is available about the desired signal and about the structure of the noise covariance matrix, we make $\alpha = 0$ and $R_w = I$ in (2.6), which leads to

$$\hat{x}^{\mathrm{DS}}(k) = \frac{a^H(\theta)}{a^H(\theta)a(\theta)}z(k) \tag{2.12}$$

i.e., to the conventional delay-and-sum (DS) beamformer.

C. Least Absolute Value Beamformer: $p = 1$

As an alternative to quadratic norms, we consider now the least absolute value or l_1 beamformer. We take, in (2.2), $d_1(\cdot;\cdot)$ to be the l_1 norm $p = 1$. In Section IV, we will show that this beamformer is capable of adjusting itself to the environment conditions and is robust when outliers are present. The general cost functional (2.2) takes the form

$$J_{l_1} = 2\sum_{n=1}^{N}\frac{|v_n^H r(k)|}{\sqrt{\lambda_n}} + \alpha x^H(k)R_x^{-1}x(k). \tag{2.13}$$

The first term in the right-hand side is the l_1 norm of the residues vector

$$r(k) = z(k) - a(\theta)x(k) \tag{2.14}$$

in the metric R_w^{-1} where

$$R_w = \sum_{n=1}^{N} v_n\lambda_n v_n^H. \tag{2.15}$$

The factor 2 is a normalizing constant. Differentiating (2.13) with respect to $x(\cdot)$ and equating to zero yields the nonlinear equation

$$\left[\alpha R_x^{-1} + a^H(\theta)Q^{-1}(k)a(\theta)\right]x(k) = a^H(\theta)Q^{-1}(k)z(k) \tag{2.16}$$

where

$$Q^{-1}(k) = \sum_{n=1}^{N}\frac{v_n v_n^H}{\sqrt{\lambda_n}|v_n^H r(k)|}. \tag{2.17}$$

Here Q^{-1} plays the role of the noise inverse kernel R_w^{-1} in (2.6). Equation (2.16) can be solved using, for example, the reweighted least squares algorithm [24]. Let $\hat{x}_i(k)$ be the solution of (2.16) at time k and iteration i; then, at iteration $i+1$

$$\hat{x}_{i+1}(k) = \frac{a^H(\theta)Q_i^{-1}(k)z(k)}{\alpha R_x^{-1} + a^H(\theta)Q_i^{-1}(k)a(\theta)} \tag{2.18}$$

where, according to (2.17) and (2.14), $Q_i^{-1}(k)$ depends on the residues vector at the ith iteration. This algorithm can be initialized using, for instance, the MVDR solution (2.11) discussed in the previous subsection. As mentioned before, the previously known kernel R_w^{-1} is here substituted by $Q^{-1}(\cdot)$, which depends on the actual value of the residues. In (2.17), $|v_n^H r(k)|$ measures the length of the component of the residues vector along the noise eigenvector v_n. Using (2.17), the numerator of (2.18) can be rewritten as

$$a^H(\theta)Q_i^{-1}(k)z(k) = \sum_{n=1}^{N}\left(\frac{\sqrt{\lambda_n}}{|v_n^H r_i(k)|}\right)\frac{\left[a^H(\theta)v_n\right]\left[v_n^H z(k)\right]}{\lambda_n}. \tag{2.19}$$

The filtering operation in (2.19) attenuates the components of the observations $v_n^H z(k)$ responsible for large residues $|v_n^H r_i(k)| \gg \sqrt{\lambda_n}$, enhancing those that best match the desired field $|v_n^H r_i(k)| \ll \sqrt{\lambda_n}$. This discussion brings out an important property of the l_1 norm solution for the beamforming problem: its capability of adjusting itself to the noise conditions. If the observation noise does not follow the assumed model, as, for example, when outliers are present, some of the residues will be large when compared with the standard deviation of the respective noise components. Equation (2.19) shows that essentially only the observation components not affected by the occurrence of outliers are used to perform the signal estimate. This is even more apparent when $R_w = \sigma_w^2 I$, where it follows that

$$a^H(\theta)Q_i^{-1}(k)z(k) = \sum_{n=1}^{N}\frac{1}{|r_{i_n}(k)|}a_n^*(\theta)z_n(k)$$

i.e., sensors where measurements lead to large residues $|r_{i_n}(k)| \gg 1$ are practically discarded by the processing.

III. Recursive Implementation of the l_1 and l_2 Beamformers

In Section II, we used the inverse approach to design l_2 and l_1 beamformers. Here, we will derive time recursive implementations of those beamformers. With no loss of generality, the following introductory discussion is presented in the l_1 norm context.

Consider the problem of reconstructing the field $x(k)$ as an l_1 inversion problem specified by the functional (2.13). This may be solved by iterative schemes, namely the gradient algorithm, where each iteration is obtained by correcting the previous estimate with the functional's gradient evaluated at the previous iteration. For the problem under consideration

$$\hat{x}_{i+1}(k) = \hat{x}_i(k) + \mu\left[-\alpha R_x^{-1}\hat{x}_i(k) + a^H(\theta)Q_i^{-1}(k)r_i(k)\right], \tag{3.20}$$

where μ is a parameter that controls the convergence of the algorithm. When the signals are slowly varying relative to the sampling period, it is conceivable that a convergent algorithm can be implemented recursively in time without a significant performance degradation. The assumption of slowly varying signals is verified in applications, such as time domain beamforming, where oversampling techniques are used [19]. Iterating on the time index k instead of the index i and grouping terms, the iterative scheme in (3.20) is written as

$$\hat{x}(k+1) = (1 - \mu\alpha R_x^{-1})\hat{x}(k) + \mu a^H(\theta)Q^{-1}(k)r(k). \tag{3.21}$$

This is a time-recursive scheme where the dynamics follows the prior knowledge about the desired signal as corrected by

the residues $r(k)$. This suggests the use of Kalman–Bucy filtering theory to design time recursive beamformers. Within this framework, the prior knowledge about the signal to be estimated is modeled using a state space representation. This is discussed in the following paragraph.

A. Signal Model

We define a low pass representation for the complex envelope of the signal which is described by a difference equation. We notice that model selection can be critical since a possible model mismatch may cause the divergence of the beamformer output. For instance, using a reduced order model in order to decrease computational complexity can be responsible for severe performance degradation. The discussion of these relevant problems, which have been addressed by several authors in a number of papers, is beyond the scope of this paper; see [1], [8], [12]–[14], [18], [25]. Nevertheless, for the important applications considered in Section I, prior knowledge of the desired signal is available, enabling the specification of an accurate signal model. Here, to avoid unnecessary complications, we proceed in the simple context of a first-order signal, whose complex envelope is specified by

$$x(k+1) = fx(k) + u(k+1), \qquad k = 0, 1, \ldots \quad (3.22)$$
$$x(0) = x_0$$

where the condition $|f| < 1$ insures stability. The initial condition x_0 is a zero mean complex random variable with variance P_0, and $u(\cdot)$ is a complex white sequence with spectral level R_u that is statistically independent of x_0. For both x_0 and $u(\cdot)$, the inphase $Re\{\cdot\}$(*Re*$\{\cdot\}$ denotes real part) and quadrature $Im\{\cdot\}$(*Im*$\{\cdot\}$ denotes imaginary part) components are statistically independent and identically distributed.

B. Self-Adjusted l_1-Recursive Beamformer

We first consider the recursive implementation of the l_1 beamformer. The l_1 inversion problem is formulated as follows: Given the set of observations $Z_{k+1} = \{z(m)\}_{m=1}^{k+1}$ and the model (3.22), determine the sequence of estimates $\{\hat{x}(m)\}_{m=0}^{k+1}$. By analogy with the Kalman–Bucy filtering theory, the l_1 cost functional is written as

$$J_{k+1} = 2\sum_{n=1}^{N} \frac{|v_n^H[z(k+1) - a(\theta)x(k+1)]|}{\sqrt{\lambda_n}} + \alpha\left[\| x(k) - \hat{x}(k) \|^2_{P^{-1}(k)} + \| u(k+1) \|^2_{R_u^{-1}}\right] \quad (3.23)$$

where $\|(\cdot)\|^2_{R^{-1}} = (\cdot)^H R^{-1}(\cdot)$, and $P(\cdot)$ is the error covariance. The problem is to compute $x(k)$, $x(k+1)$, and $u(k+1)$ that minimize (3.23) subject to the constraint (3.22). We use Lagrange multipliers. Let L_{k+1} be the Lagrangean

$$L_{k+1} = J_{k+1}(x_{k+1}, x_k, u_{k+1}) + 2\mathrm{Re}\{\nu^*[x(k+1) - fx(k) - u(k+1)]\}$$

where ν is the Lagrange multiplier. Equating to zero the partial derivatives of the Lagrangean with respect to $x(k)$, $x(k+1)$, and $u(k+1)$

$$\begin{aligned} \alpha P^{-1}(k)[x(k) - \hat{x}(k)] - f\nu^* &= 0 \\ -a^H(\theta)Q^{-1}(k+1)[z(k+1) - a(\theta)x(k+1)] + \nu^* &= 0 \\ \alpha R_u^{-1}u(k+1) - \nu^* &= 0. \end{aligned} \quad (3.24)$$

These are necessary conditions for the existence of a minimum. In (3.24), $Q^{-1}(\cdot)$ is as defined by (2.17). This nonlinear system of equations can be linearized by approximating the residues (2.14) by

$$r_k(k+1) = z(k+1) - a(\theta)\hat{x}_k(k+1)$$

where $\hat{x}_k(k+1)$ is the predicted value of $x(k+1)$ given the previous estimate $\hat{x}(k) = E\{x(k)|Z_k\}$:

$$\hat{x}_k(k+1) = E\{x(k+1)|Z_k\} = f\hat{x}(k).$$

Using this linearization, the solution of (3.24) implements the l_1 beamformer by a time-recursive algorithm, here denoted as the l_1-recursive beamformer.

1) **Initialization:**

$$\hat{x}(0) = 0$$
$$P(0) = P_0 = I$$

2) **Prediction:**

$$\hat{x}_k(k+1) = f\hat{x}(k) \quad (3.25)$$
$$P_k(k+1) = |f|^2P(k) + R_u \quad (3.26)$$

3) **Residues and adjusted gain:**

$$r_k(k+1) = z(k+1) - a(\theta)\hat{x}_k(k+1) \quad (3.27)$$
$$Q^{-1}(k+1) = \sum_{n=1}^{N} \frac{v_n v_n^H}{\sqrt{\lambda_n}|v_n^H r_k(k+1)|} \quad (3.28)$$
$$K^H(k+1) = \frac{\alpha^{-1}P_k(k+1)a^H(\theta)Q^{-1}(k+1)}{1 + \alpha^{-1}P_k(k+1)a^H(\theta)Q^{-1}(k+1)a(\theta)} \quad (3.29)$$

4) **Filtering:**

$$\hat{x}(k+1) = \hat{x}_k(k+1) + K^H(k+1)r_k(k+1) \quad (3.30)$$

5) **Updating of the error covariance:**

$$P(k+1) = [1 - K^H(k+1)a(\theta)]P_k(k+1) \times [1 - a^H(\theta)K(k+1)] + K^H(k+1)R_wK(k+1) \quad (3.31)$$

where $P(\cdot)$ denotes the error covariance conditioned on the predicted residues.

Equations (3.27)–(3.30) show the property of the l_1 beamformer of adjusting itself to high values of the components of the residues, as mentioned before.

The derivation of this algorithm was based on the assumption of uncorrelated observation noise and signal. If the observation noise is correlated with the desired signal, as it is the case when multipath propagation occurs, the algorithm can be easily modified using the well-known *augmented* state vector technique [14].

C. l_2-Recursive Beamformer

Model (3.22) may also be used to derive a time-recursive implementation for the l_2 beamformer. The functional to be minimized subject to the model restriction (3.22) is now

$$J_{k+1} = \|z(k+1) - a(\theta)x(k+1)\|^2_{R_w^{-1}} + \alpha\Big[\|x(k) - \hat{x}(k)\|^2_{P^{-1}(k)} + \|u(k+1)\|^2_{R_u^{-1}}\Big]. \tag{3.32}$$

The result of this minimization problem is specified by a discrete Kalman–Bucy filter matched to the signal model (3.22).

l_2-Recursive Beamformer:

1) **Initialization:**

$$\hat{x}(0) = 0$$
$$P(0) = P_0 = I$$

2) **Prediction:**
Use (3.25) and (3.26).

3) **Kalman gain:**

$$K^H(k+1) = \frac{\alpha^{-1}P_k(k+1)a^H(\theta)R_w^{-1}(k+1)}{1 + \alpha^{-1}P_k(k+1)a^H(\theta)R_w^{-1}(k+1)a(\theta)} \tag{3.33}$$

4) **Filtering:**
Use (3.30).

5) **Updating of the error covariance:**

$$P(k+1) = \big[1 - K^H(k+1)a(\theta)\big]P_k(k+1) + (1-\alpha)K^H(k+1)R_wK(k+1) \tag{3.34}$$

The structure of this algorithm is similar to that of the l_1-recursive beamformer. There is, however, an important difference. When comparing (3.33) with (3.29), we see that the l_2-recursive beamformer lacks the adjustable feature of the l_1 beamformer since the Kalman gain in (3.33) is completely specified by the prior knowledge about the observation noise.

IV. Performance Analysis

In this section, we analyze the performance of the l_2 and l_1 beamformers. First, we study the behavior of the MMSE beamformer in the presence of correlated arrivals. We show that the MMSE beamformer uses this correlation to improve the output signal to noise ratio, in contrast with the MVDR beamformer, which exhibits signal cancelation [10], [20], [21]. Second, we compare the performance of the l_2 and l_1 beamformers. Two situations are considered: 1) directional signal in white noise and 2) directional signal in white noise and unexpected impulsive noise. In both cases, the statistics of the background white noise and the signal model are assumed known. This study emphasizes the robustness of the l_1 approach when unexpected noise conditions occur, like the impulsive noise field. We show that, in the first case 1), the two beamformers have similar behavior, whereas in situation 2), they behave quite differently: The l_2 beamformer is strongly affected by the impulsive noise, whereas the l_1 structure strongly attenuates the unexpected noise impulses.

We restrict our attention to the case of linear and uniform arrays. In this case, the Vandermonde steering vectors $a(\theta)$ specifying the directions of arrival are defined by

$$a(\theta) = \Big[1, e^{-j\omega_0\tau(\theta)}, \ldots, e^{-j\omega_0(N-1)\tau(\theta)}\Big]^T \tag{4.35}$$

with

$$\tau(\theta) = \frac{d}{c}\sin(\theta) \tag{4.36}$$

where

- d intersensors distance
- c propagation velocity
- θ angle of arrival measured from broadside.

The observations are

$$z(k) = a(\theta)x(k) + s(k) + w(k) \tag{4.37}$$

where $x(\cdot)$ is the desired signal, $s(\cdot)$ models disturbances such as a directional interference or unexpected noise, and $w(\cdot)$ is an independent space/time white noise field with covariance matrix

$$R_w = \sigma_w^2 I. \tag{4.38}$$

A. Correlated Arrivals: MMSE Beamformer

In this section, we concentrate on the behavior of the MMSE beamformer when correlated arrivals are observed. For this case, vector $s(\cdot)$ in (4.37) is

$$s(k) = a(\theta_i)x_i(k) \tag{4.39}$$

where $x_i(\cdot)$ is a directional interference arriving from θ_i. The signal and interference covariances are R_x and R_i, respectively. With generality, we assume that signal and interference are correlated, the correlation factor being defined by

$$\rho = \frac{E\{x(k)x_i^*(k)\}}{\sqrt{R_xR_i}}. \tag{4.40}$$

The output of the MMSE beamformer is (see (2.7))

$$\hat{x}^{\mathrm{MMSE}}(k) = R_{xz}R_z^{-1}z(k) \tag{4.41}$$

which, with our assumptions and after some algebra, yields

$$\hat{x}^{\mathrm{MMSE}}(k) = \frac{1}{N}\left(\frac{\frac{\sigma_w^2}{N}R_x + (1-|\rho|^2)R_xR_i}{\Delta}a^H(\theta) + \frac{\frac{\sigma_w^2}{N}\rho\sqrt{R_xR_i} - \beta^*(1-|\rho|^2)R_xR_i}{\Delta}a^H(\theta_i)\right)z(k) \tag{4.42}$$

where

$$\Delta = \left(\frac{\sigma_w^2}{N}\right)^2 + \left(\frac{\sigma_w^2}{N}\right)\Big[R_x + R_i + 2\sqrt{R_xR_i}\mathrm{Re}\{\beta\rho\}\Big] + \big(1-|\beta|^2\big)\big(1-|\rho|^2\big)R_xR_i \tag{4.43}$$

and

$$\beta = \frac{1}{N} a^H(\theta_i) a(\theta) = |\beta| e^{j\phi_\beta}. \tag{4.44}$$

The parameter β measures the spatial coherence between the arrivals. Using (4.42), (4.37), and (4.39), it can be shown that the MMSE beamformer output error covariance $P^{\text{MMSE}} = E\{|x(k) - \hat{x}^{\text{MMSE}}(k)|^2\}$ is

$$P^{\text{MMSE}} = \frac{\sigma_w^2}{N} \frac{\frac{\sigma_w^2}{N} R_x + (1 - |\rho|^2) R_x R_i}{\Delta}. \tag{4.45}$$

These are new analytical results that can be used to study the behavior of the MMSE beamformer. We will consider two limiting cases: i) uncorrelated ($\rho = 0$) and ii) coherent ($|\rho| = 1$) arrivals.

1) Uncorrelated Arrivals: We assume uncorrelated arrivals, i.e., $\rho = 0$ (see (4.40)). Let the signal/noise and the interference/noise ratios be defined by

$$\text{SNR} = \frac{R_x}{(\sigma_w^2/N)} \tag{4.46}$$

$$\text{INR} = \frac{R_i}{(\sigma_w^2/N)}. \tag{4.47}$$

Then, from (4.42)–(4.44), we can compute the values of the MMSE beampattern at the look (θ) and interference (θ_i) directions, which are

$$B(\theta) = \frac{\text{SNR}}{1 + \text{SNR}} \frac{1 - |\beta|^2 \frac{\text{INR}}{1+\text{INR}}}{1 - |\beta|^2 \frac{\text{INR}}{1+\text{INR}} \frac{\text{SNR}}{1+\text{SNR}}} \tag{4.48}$$

and

$$B(\theta_i) = \frac{1}{1 + \text{INR}} \frac{\text{SNR}}{1 + \text{SNR}} \frac{|\beta|}{1 - |\beta|^2 \frac{\text{INR}}{1+\text{INR}} \frac{\text{SNR}}{1+\text{SNR}}} \tag{4.49}$$

respectively. Dividing (4.48) by (4.49)

$$\frac{B(\theta)}{B(\theta_i)} = (1 + \text{INR}) \frac{1 - |\beta|^2 \frac{\text{INR}}{1+\text{INR}}}{|\beta|} \tag{4.50}$$

we conclude that, at the interference direction, the MMSE beamformer puts a null whose depth increases with INR. This behavior is similar to that of both the MVDR and MNPDR beamformers. However, and contrarily to what happens with these beamformers, the gain of the MMSE beamformer at the look direction is no longer unity (see (4.48)). This is balanced by a stronger noise rejection that leads to a smaller output error power, as we now show. In fact, for the case under study, (4.45) takes the form

$$P^{\text{MMSE}} = \frac{\sigma_w^2}{N} \frac{\text{SNR}}{1 + \text{SNR}} \frac{1}{1 - |\beta|^2 \frac{\text{INR}}{1+\text{INR}} \frac{\text{SNR}}{1+\text{SNR}}}. \tag{4.51}$$

On the other hand, using (2.11), (4.37), and (4.39), we can compute the output error power of the MVDR and MNPDR[1] beamformers as

$$P^{\text{MVDR}} = P^{\text{MNPDR}} = \frac{\sigma_w^2}{N} \frac{1}{1 - |\beta|^2 \frac{\text{INR}}{1+\text{INR}}}. \tag{4.52}$$

[1] We recall that for this case, i.e., uncorrelated arrivals, the MVDR and MNPDR beamformers are equivalent. Hence, $P^{\text{MVDR}} = P^{\text{MNPDR}}$.

Dividing (4.51) by (4.52), the error power

$$P^{\text{MMSE}} \leq \frac{\text{SNR}}{1 + \text{SNR}} P^{\text{MVDR}} = \frac{\text{SNR}}{1 + \text{SNR}} P^{\text{MNPDR}} \tag{4.53}$$

confirming the above assertion.

2) Coherent Arrivals: We consider the other limiting case where

$$\rho = e^{j\phi_\rho} \tag{4.54}$$

i.e., except for a phase difference, signal, and interference differ only on their power levels. The output of the MMSE beamformer (see (4.42) and (4.43)) is

$$\hat{x}^{\text{MMSE}}(k) = \frac{1}{N} \frac{\text{SNR} a^H(\theta) + \sqrt{\text{SNR}\,\text{INR}} e^{j\phi_\rho} a^H(\theta_i)}{1 + \text{SNR} + \text{INR} + 2\sqrt{\text{SNR}\,\text{INR}} |\beta| \text{Re}\{e^{j(\phi_\rho + \phi_\beta)}\}} z(k) \tag{4.55}$$

where we used definitions (4.46) and (4.47). From (4.55), we compute the values of the MMSE beampattern at the look and interference directions. Doing so, we obtain the ratio

$$\frac{B(\theta)}{B(\theta_i)} = \frac{\left|1 + \sqrt{\frac{\text{INR}}{\text{SNR}}} |\beta| e^{j(\phi_\beta + \phi_\rho)}\right|}{\left||\beta| + \sqrt{\frac{\text{INR}}{\text{SNR}}} e^{j(\phi_\beta + \phi_\rho)}\right|}. \tag{4.56}$$

3) Orthogonal or Well-Separated Arrivals: For orthogonal or well separated arrivals ($|\beta| \simeq 0$), ratio (4.56) is determined by SNR/INR. In distinction with what happens in the case of uncorrelated arrivals of the last paragraph, the MMSE beamformer exhibits two peaks (one at the look direction and the other at the interference direction) whose amplitudes depend on SNR and INR. Instead of rejecting the interference, the MMSE beamformer uses its correlation with the desired signal to combine coherently the two replicas.

4) Close Arrivals: For close arrivals ($|\beta| \simeq 1$), the gains of the MMSE beamformer at the two directions θ and θ_i are practically equal. For a better understanding of what happens in this situation, we analyze the expression of the output error power. With $|\beta| \simeq 1$ and using (4.44) and (4.54), (4.45) yields

$$P^{\text{MMSE}} = \frac{\sigma_w^2}{N} \frac{\text{SNR}}{1 + \text{SNR} + \text{INR} + 2\sqrt{\text{SNR}\,\text{INR}} \cos(\phi_\rho)}. \tag{4.57}$$

In the case of zero observation noise ($\sigma_w^2 = 0$), $P^{\text{MMSE}} = 0$. This means that in the absence of observation noise, the output of the MMSE beamformer gives the actual value of the desired signal. This behavior is quite different from that of the MVDR beamformer, which, for this case, cancels the signal of interest [21]. Although signal cancellation does not occur when MNPDR and DS beamformers are used, the performance that is obtained is poorer than that of the MMSE beamformer. Noticing that, with regard to the MNPDR beamformer, (4.52) is also verified for correlated arrivals, it can be easily verified that in the present situation, i.e., $\beta \simeq 1$ and $\sigma_w^2 = 0$, the error covariance at the output of the MNPDR beamformer is approximately given by the covariance of the coherent interference, R_i. This is also true for the DS beamformer. As

we see from (4.57), the behavior of the MMSE beamformer depends on the particular value of the phase difference ϕ_ρ. Since

$$-1 \leq \cos(\phi_\rho) \leq 1 \tag{4.58}$$

we establish the bounds

$$\frac{\sigma_w^2}{N}\frac{\text{SNR}}{1+\left(\sqrt{\text{SNR}}+\sqrt{\text{INR}}\right)^2} \leq P^{\text{MMSE}} \leq \frac{\sigma_w^2}{N}\frac{\text{SNR}}{1+\left(\sqrt{\text{SNR}}-\sqrt{\text{INR}}\right)^2}. \tag{4.59}$$

The lower and upper bounds are achieved when signal and interference are inphase and 180° out of phase, respectively. We analyze this expression for three relative levels of SNR and INR.

Case 1 : SNR $\gg$ INR: Under this condition, the two bounds in (4.59) are approximately equal, which means that

$$P^{\text{MMSE}} = \frac{\sigma_w^2}{N}\frac{\text{SNR}}{1+\text{SNR}}. \tag{4.60}$$

This is to be expected since it corresponds to the situation where the interference is absent.

Case 2 : SNR $\simeq$ INR: Using this assumption in (4.59) yields

$$\frac{\sigma_w^2}{N}\frac{\text{SNR}}{1+4\text{SNR}} \leq P^{\text{MMSE}} \leq R_x. \tag{4.61}$$

When $\phi_\rho = 180°$ (upper bound in (4.61), the error power at the output of the MMSE beamformer equals the signal power R_x. This means that, for coherent close arrivals approximately 180° out of phase, the MMSE output power is zero. However, we are not talking about array signal cancellation but rather of an effective absence of the signal in the received waveform. In fact, the assumed conditions are equivalent to saying that at each sensor the array is observing only noise. When, at each sensor, the incoming coherent signals are added instead of being subtracted, P^{MMSE} decreases significantly and approximates the lower bound in (4.61).

Case 3: SNR $\ll$ INR: As in case 1, the two bounds in (4.59) are approximately equal:

$$P^{\text{MMSE}} = \frac{\sigma_w^2}{N}\frac{\text{SNR}}{1+\text{INR}}. \tag{4.62}$$

The output error power of the MMSE beamformer decreases when INR increases.

Fig. 1 illustrates the behavior of both the MMSE and MNPDR beamformers, as predicted by (4.51), (4.52), and the bounds in (4.59), for the case of spatially close signal and interference ($|\beta| \simeq 1$). We can see that the MMSE beamformer outperforms the MNPDR beamformer in all situations, particularly for the case of coherent arrivals.

The analysis presented enables us to conclude that the MMSE beamformer presents a superior performance when compared to the MVDR, MNPDR, and DS beamformers, its major advantage resulting from the coherent combination of correlated arrivals in multipath scenarios. In these situations, the MVDR beamformer exhibits signal cancellation, whereas the MNPDR (DS) beamformer rejects (attenuates) the correlated replicas of the desired signal as if they did not convey relevant information.

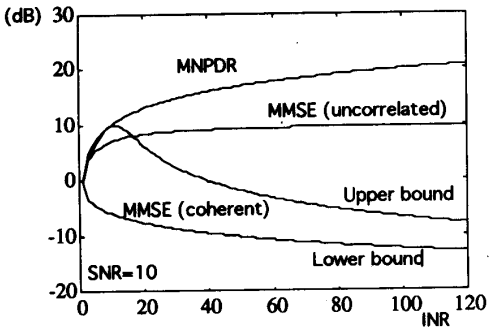

(a)

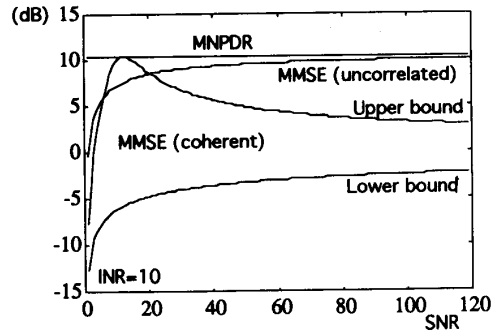

(b)

Fig. 1. Output error power: (a) As a function of INR; (b) as a function of SNR.

B. Directional Signal in White Noise

In this section, we analyze the performance of both the l_1 and l_2 beamformers when the only disturbance in the measurements is white, i.e., in (4.37), the component $s(\cdot) \equiv 0$. The signal model (3.22) is assumed known. Below, quantities that are subscripted by l_1 refer to the l_1 beamformer and likewise for l_2.

1) First-Order Analysis—Bias: We compute the bias of the l_1 and l_2 beamformers. Let the errors at the output of the l_1 and l_2 beamformers be $\varepsilon_{l_1}(\cdot)$ and $\varepsilon_{l_2}(\cdot)$, respectively. From (A.83) and (A.84) in Appendix A, and using the facts that $E\{u(\cdot)\} = 0$ and $E\{w(\cdot)\} = 0$, we get the difference equations

$$E\{\varepsilon_{l_2}(k+1)\} = \frac{\alpha}{\alpha + N\frac{P_k(k+1)_{l_2}}{\sigma_w^2}} f E\{\varepsilon_{l_2}(k)\} \tag{4.63}$$

and

$$E\{\varepsilon_{l_1}(k+1)|\{r_m(m+1)\}_{m=0}^{k}\} = \frac{\alpha f}{\alpha + P_k(k+1)_{l_1}\sum_{n=1}^{N}|r_{k_n}(k+1)|^{-1}} \cdot E\{\varepsilon_{l_1}(k)|\{r_m(m+1)\}_{m=0}^{k-1}\}. \tag{4.64}$$

Since $|f| < 1$ and $\alpha > 0$, (4.63) and (4.64) are asymptotically stable difference equations so that

$$\forall \varepsilon_{l_2}(0) : |E\{\varepsilon_{l_2}(k+1)\}| \underset{k\to\infty}{\longrightarrow} 0 \tag{4.65}$$

and

$$\forall \varepsilon_{l_1}(0) : |E\{\varepsilon_{l_1}(k+1)|\{r_m(m+1)\}_{m=0}^{k}\}| \underset{k\to\infty}{\longrightarrow} 0 \tag{4.66}$$

i.e., the l_2 and l_1 beamformers are asymptotically unbiased.

Notice that the convergence rate in the l_1 case is directly controlled by the absolute value of the predicted residues. Smaller values of the predicted residues induce a faster convergence rate. On the contrary, the convergence rate of the bias at the output of the l_2 beamformer is prespecified by the assumed statistics.

2) Second-Order Analysis—Error Covariance: For the purpose of simplicity, assume that $\alpha = 0$, i.e., that there is no prior knowledge about the desired field $x(\cdot)$. From (A.85) and (A.86), we get

$$P(k+1)_{l_2} = \frac{\sigma_w^2}{N} \tag{4.67}$$

and

$$P(k+1)_{l_1} = \sigma_w^2 \frac{\sum_{n=1}^{N} |r_{k_n}(k+1)|^{-2}}{(\sum_{n=1}^{N} |r_{k_n}(k+1)|^{-1})^2} \tag{4.68}$$

respectively. Let $r_{\min}$ and $r_{\max}$ be, respectively, the minimum and the maximum values of the lengths of the predicted residues at time $k+1$ over all the array sensors. The conditional error covariance (4.68) takes values in the interval

$$\frac{r_{\min}^2}{r_{\max}^2}\frac{\sigma_w^2}{N} \le P(k+1)_{l_1} \le \frac{r_{\max}^2}{r_{\min}^2}\frac{\sigma_w^2}{N}. \tag{4.69}$$

In the weak noise case (small values of σ_w^2), it is likely that the dispersion of the predicted residues is small, i.e., $r_{\min} \simeq r_{\max}$. Hence, with high probability

$$P(k+1)_{l_1} \simeq P(k+1)_{l_2}. \tag{4.70}$$

In other words, for small values of the observation noise power, the l_2-recursive and the l_1-recursive beamformers present, with high probability, similar values for the conditional covariance of the output error. In Section V, we will verify by simulations this to be in fact the case.

Using the inequality

$$\forall k, \sum_{n=1}^{N} |r_{k_n}(k+1)|^{-2} < \left(\sum_{n=1}^{N} |r_{k_n}(k+1)|^{-1}\right)^2 \tag{4.71}$$

and (4.68), we can write

$$\frac{r_{\min}^2}{r_{\max}^2}\frac{\sigma_w^2}{N} \le P(k+1)_{l_1} < \sigma_w^2. \tag{4.72}$$

Even when the noise is strong, in which case the residues with a large dispersion are typical, the conditional error covariance $P(k+1)_{l_1}$ is upper bounded by the observation noise power. No such constraint exists for $P(k+1)_{l_2}$; therefore, depending on the noise samples, events like

$$P(k+1)_{l_1} \le P(k+1)_{l_2} \tag{4.73}$$

have nonzero probability. This observation will be used in the following subsection.

C. Unexpected Impulsive Noise

We study here the behavior of the l_1 and l_2 beamformers when unexpected impulsive noise occurs. This may represent unmodeled failures of sensors or spiky noise not accounted for in the model. This is taken care of by introducing the term $s(\cdot)$ in (4.37) when analyzing the beamformers but designing these assuming that no component $s(\cdot)$ is present in (4.37), i.e., that the only disturbance present is white noise. This means that the observed measurements do not follow the conditions under which the beamformers were designed. We analyze the situation where unexpected impulsive noise is present.

1) Model of the Impulsive Noise Field: At each sensor, the impulsive noise sample $s_n(\cdot)$ is defined by the product of three jointly independent random variables (r.v.): a time-indexed Bernoulli r.v. $\beta(\cdot)$, a spatially indexed Bernoulli r.v. Γ_n, and a space/time indexed zero-mean Gaussian r.v. $\gamma_n(\cdot)$ with variance σ^2. The Bernoulli variables $\beta(\cdot)$ and Γ_n control the instants and sensors at which there may occur impulses. If p and $p_{\#}$ are the probabilities of the events $\beta(\cdot) = 1$ and $\Gamma_n = 1$, respectively, then the probability of an impulse occurring is $p\,p_{\#}$. When this happens, the unexpected impulse $s_n(\cdot) = \gamma_n(\cdot)$ is characterized by the statistics of the Gaussian r.v. $\gamma_n(\cdot)$. This construction of the impulsive noise is such that the total noise field, i.e., background white noise $w(\cdot)$ plus impulsive noise $s(\cdot)$, follows the well-known Gauss-Gauss mixture model.

2) l_1 Beamformer: Using (A.87), we get the difference equation

$$\begin{aligned} &E\{\varepsilon_{l_1}(k+1)|\{r_m(m+1)\}_{m=0}^{k}\} \\ &\quad = \frac{\alpha f}{\alpha + P_k(k+1)_{l_1}\sum_{n=1}^{N}|r_{k_n}(k+1)|^{-1}} \\ &\qquad \times E\{\varepsilon_{l_1}(k)|\{r_m(m+1)\}_{m=0}^{k-1}\}. \end{aligned} \tag{4.74}$$

This result is formally analogous to (4.64), except that here, the predicted residues have an additional term $s(\cdot)$. Nevertheless, since (4.74) is still an asymptotically stable difference equation, the result (4.66) remains valid. This means that in spite of the disturbance $s(\cdot)$ not accounted for in the observations model, the l_1-recursive beamformer is asymptotically unbiased.

Consider again the case $\alpha = 0$. From (A.87), we have

$$\begin{aligned} &\varepsilon_{l_1}(k+1) \\ &\quad = -\frac{\sum_{n=1}^{N} a_n^*(\theta)|r_{k_n}(k+1)|^{-1}[w_n(k+1)+s_n(k+1)]}{\sum_{n=1}^{N}|r_{k_n}(k+1)|^{-1}}. \end{aligned} \tag{4.75}$$

Suppose that this is the first-time impulses occur, after a long absence of impulses, is at time $k+1$, i.e., that $\beta(k+1) = 1$ and that p is sufficiently small so that it is reasonable to assume

$$\ldots \beta(k-2), \beta(k-1), \beta(k) = 0.$$

When the unmodeled noise is much stronger than the background noise at the malfunctioning sensors, i.e.

$$\sigma^2 \gg \sigma_w^2 \tag{4.76}$$

the probability of the event

$$|s_n(k+1)| \gg |w_n(k+1)| \tag{4.77}$$

is high. Under these conditions, the predicted residues in those malfunctioning sensors have large absolute values, and (4.75) can be approximated with high probability by

$$\varepsilon_{l_1}(k+1) \simeq -\frac{\sum_{N-L} a_n^*(\theta)|r_{k_n}(k+1)|^{-1}w_n(k+1)}{\sum_{N-L}|r_{k_n}(k+1)|^{-1}} \tag{4.78}$$

where L is the number of failing sensors. The error covariance conditioned on the residues is then

$$\sigma^2_{\varepsilon_{l_1}}(k+1) \simeq \sigma_w^2 \frac{\sum_{N-L}|r_{k_n}(k+1)|^{-2}}{\left(\sum_{N-L}|r_{k_n}(k+1)|^{-1}\right)^2}. \tag{4.79}$$

This formula accounts for those sensors whose residues depend mainly on the background noise. As in Section IV-B (see (4.70) and (4.67)), we conclude that

$$\sigma^2_{\varepsilon_{l_1}}(k+1) \simeq \frac{\sigma_w^2}{N-L}. \tag{4.80}$$

In the presence of strong impulsive noise (see (4.76)), the error covariance at the output of the l_1-recursive beamformer depends essentially on the power of the background noise. If the probability of the occurrence of impulses is small, then the likelihood that only a small number L of sensors fails is large and (4.80) approximates (4.70), i.e., the l_1-recursive beamformer behaves much like in the background-noise-only case. This result shows the robustness of this algorithm to the presence of outliers.

3) l_2 Beamformer: Assuming the conditions of the previous paragraph, we can conclude that the error at the output of the l_2-recursive beamformer is also asymptotically unbiased and that its covariance is

$$\sigma^2_{\varepsilon_{l_2}}(k+1) \simeq \frac{\sigma_w^2}{N} + \frac{pp_{\#}\sigma^2}{N}. \tag{4.81}$$

When the impulsive noise is strong, the second term dominates the first in equation (4.81), and therefore, $\sigma^2_{\varepsilon_{l_2}}$ depends mainly on the power of the unexpected impulses. This is in sharp distinction with (4.80) and says that the performance of the l_2 structure deteriorates sharply when outliers are present.

V. Simulations

In this section, we discuss results of simulations performed under distinct scenarios representing the situations considered in the last section. The observations are synthesized using the model (4.39). The involved directional signals follow the 1st order discrete state representation (3.22).

TABLE I
SCENARIO 1

$\alpha = 1$	Direction (degrees)	Mean Power (linear unities)
Signal	0	1
Interference 1	−15	1
Interference 2	10	1
Noise	—	0.5

A. Performance in White Noise and Directional Interferences

Here, we study the behavior of both the l_2 and l_1 beamforming algorithms in the presence of directional interferences as well as their performance as a function of the background white noise power. We consider a situation where a coherent replica of the desired signal is present.

Scenario 1: Consider a linear array of $N = 10$ equally spaced sensors. The intersensors distance is half the wavelength. Table I specifies the conditions of the experiment. The desired signal is observed at broadside ($\theta = 0°$) in superposition with two directional interferences arriving from $\theta = -15°, 10°$, and 3 dB stronger than the white noise field. The source at $\theta = -15°$ is a coherent replica of the desired signal. The source signal and the interference at $\theta = 10°$ are uncorrelated.

Fig. 2 depicts a phase plane representation of the estimation error, i.e., quadrature component versus inphase component. The location of the gravity center of the spot determines the expected value of the error, whereas its covariance can be qualitatively evaluated by the concentration of probability mass. An estimate of the error covariance is also presented. Results of the same experiment performed with the l_1-recursive algorithm are shown in Fig. 3. We observe that the two algorithms have a comparable behavior. In particular, notice the similarity between the phase plane representations of the error, confirming the analytical conclusions obtained in Section IV-B. Fig. 2(b) shows the beampattern of the l_2 recursive beamformer for a look direction $\theta = 0°$. This was computed using the time average of the Kalman gains as array coefficients. Notice that, as predicted by the analysis, the l_2 beamformer exhibits two main peaks corresponding to the presence of two well-separated coherent replicas of the desired signal and a null at the direction of the uncorrelated interference.

B. Performance in the Presence of Impulsive Noise

In this section, the assumed observations are disturbed by an unexpected impulsive noise field.

Scenario 2: The conditions of scenario 1 are retained. Table II specifies the parameters characterizing the impulsive noise term. Fig. 4 shows a typical record of the magnitude of the observations process in different array sensors. Notice the occurrence of high amplitude impulses contrasting with the typical values of the observations.

In Figs. 5 and 6, we show the results obtained for the l_2-recursive and l_1-recursive algorithms, respectively. Notice the factor of ten difference of scales in Figs. 5(b) and 6(b),

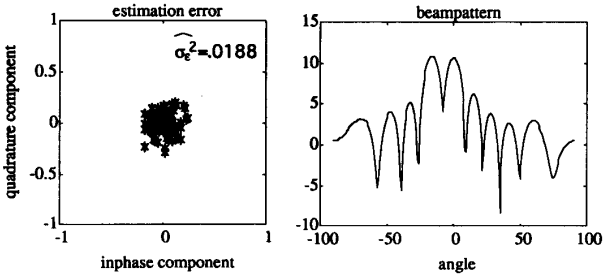

Fig. 2. l_2-recursive beamformer: (a) Phase plane representation of the error; (b) beampattern.

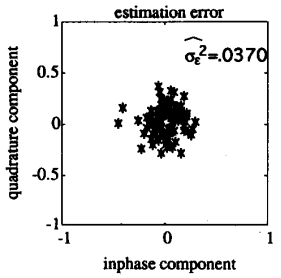

Fig. 3. l_2-recursive beamformer: Phase plane representation of the error.

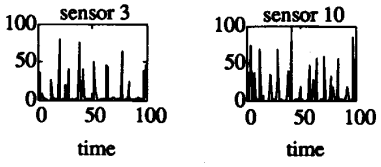

Fig. 4. Magnitude of the observations at different sensors.

showing clearly that the input impulses are replicated at the output of the l_2 beamformer, while they are practically eliminated in the estimate provided by the l_1 beamformer. As predicted by the analysis, the estimated error power at the output of the l_1 beamformer is much lower than that of the l_2 beamformer, illustrating its robustness with respect to the unmodeled impulsive noise term. On the contrary, the impulsive noise strongly affects the performance of the l_2 structure. For this case, the estimated error power is of the same order of magnitude of the approximated result obtained in Section IV; see (4.81).

VI. Conclusion

In this paper, we considered the design of beamforming structures using the inverse problem approach. Within this framework, the goal is to obtain a space/time processor that yields the best waveform estimate, given a set of noisy spatial and temporal measurements and according to some prespecified optimization criterion. Two kinds of inversion strategies were considered based on l_2 and l_1 norms.

Using this approach, we showed that the general solution for the l_2 beamforming problem is provided by the MMSE beamformer. We developed the l_1 beamformer and emphasized its adaptive characteristics. Time-recursive algorithms for both the l_1 and l_2 beamformers were derived using the Kalman–Bucy filtering theory.

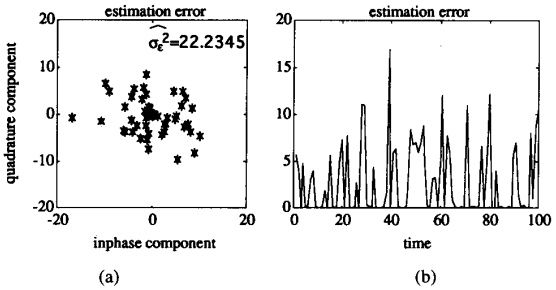

Fig. 5. l_2-recursive beamformer in impulsive noise: (a) Phase plane representation of the error; (b) time evolution of the error.

TABLE II
SCENARIO 2

Impulsive Noise
$p = 0.4$
$p_{\#} = 0.4$
$\sigma^2 = 2500$

The paper studies the performance of these algorithms, showing that in the Gaussian noise case, both beamformers have identical behaviors. We then studied the MMSE beamformer in the presence of correlated arrivals. This beamformer uses in a constructive way the correlation between the replicas. This is in distinction with the MVDR beamformer, which suffers from the well-known effect of signal cancellation and contrasts with the MNPDR (DS) beamformer, which nulls (attenuates) the correlated arrivals. Finally, we compared the l_1 and l_2 beamformers when unexpected impulsive noise is present. Although the l_2 beamformer performance deteriorates significantly, the l_1 beamformer due to its adjustable nature is quite robust, essentially discarding the information provided by the failing sensors. The simulation results confirm quite nicely the analytical results.

Appendix A
Output Error of l_1 and l_2 Beamformers

Let

$$\varepsilon(k+1) = x(k+1) - \hat{x}(k+1) \tag{A.82}$$

be the error at the beamformer's output at time $k+1$. In (4.37), assume that $s(\cdot) \equiv 0$. The error $\varepsilon_{l_2}(k+1)$ at the output of the l_2 beamformer can be computed using (3.22) together with (3.30), (3.33), (A.82), and (3.27):

$$\varepsilon_{l_2}(k+1) = \frac{\alpha}{\alpha + N\frac{P_k(k+1)_{l_2}}{\sigma_w^2}}[f\varepsilon_{l_2}(k) + u(k+1)] - \frac{\frac{P_k(k+1)_{l_2}}{\sigma_w^2}}{\alpha + N\frac{P_k(k+1)_{l_2}}{\sigma_w^2}} a^H(\theta)w(k+1). \tag{A.83}$$

$$P(k+1)_{l_1} = \left[\frac{\alpha}{\alpha + P_k(k+1)_{l_1}\sum_{n=1}^{N}|r_{k_n}(k+1)|^{-1}}\right]^2 P_k(k+1)_{l_1} + \left[\frac{P_k(k+1)_{l_1}}{\alpha + P_k(k+1)_{l_1}\sum_{n=1}^{N}|r_{k_n}(k+1)|^{-1}}\right]^2 \times \sum_{n=1}^{N}\frac{\sigma_w^2}{|r_{k_n}(k+1)|^2}, \quad \text{(A.86)}$$

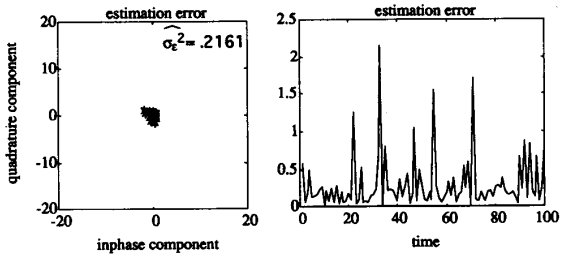

(a) (b)

Fig. 6. l_1-recursive beamformer in impulsive noise: (a) Phase plane representation of the error; (b) time evolution of the error.

Proceeding in a similar way, the error $\varepsilon_{l_1}(k+1)$ at the output of the l_1 beamformer is

$$\varepsilon_{l_1}(k+1) = \frac{\alpha}{\alpha + P_k(k+1)_{l_1}\sum_{n=1}^{N}|r_{k_n}(k+1)|^{-1}} \times [f\varepsilon_{l_1}(k) + u(k+1)] - \frac{P_k(k+1)_{l_1}}{\alpha + P_k(k+1)_{l_1}\sum_{n=1}^{N}|r_{k_n}(k+1)|^{-1}} \times \sum_{n=1}^{N} a_n^*(\theta)|r_{k_n}(k+1)|^{-1}w_n(k+1). \quad \text{(A.84)}$$

In (A.84), $r_{k_n}(k+1)$ is the predicted value of the residue at sensor n. Recall that with respect to the l_1-recursive beamformer, $P_k(k+1)_{l_1}$ and $P(k)_{l_1}$ must be interpreted as error variances conditioned on the sequence of predicted residues $\{r_m(m+1)\}_{m=0}^{k}$.

From (A.83) and (A.84), it is straightforward to find the error variance at the output of the l_2 and l_1 recursive beamformers, which are, respectively

$$P(k+1)_{l_2} = \left[\frac{\alpha}{\alpha + N\frac{P_k(k+1)_{l_2}}{\sigma_w^2}}\right]^2 P_k(k+1)_{l_2} + \left[\frac{P_k(k+1)_{l_2}}{\alpha + N\frac{P_k(k+1)_{l_2}}{\sigma_w^2}}\right]^2 N\sigma_w^2, \quad \text{(A.85)}$$

and (A.86), which appears at the top of the page.

When the beamformer's input is affected by a nonzero independent disturbance $s(\cdot)$, the error at the output of the l_1-recursive beamformer is

$$\varepsilon_{l_1}(k+1) = \frac{\alpha}{\alpha + P_k(k+1)_{l_1}\sum_{n=1}^{N}|r_{k_n}(k+1)|^{-1}} \times [f\varepsilon_{l_1}(k) + u(k+1)] - \frac{P_k(k+1)_{l_1}}{\alpha + P_k(k+1)_{l_1}\sum_{n=1}^{N}|r_{k_n}(k+1)|^{-1}} \times \sum_{n=1}^{N}\frac{a_n^*(\theta)[w_n(k+1) + s_n(k+1)]}{|r_{k_n}(k+1)|}. \quad \text{(A.87)}$$

REFERENCES

[1] M. Aoki, *State Space Modeling of Time Series*. New York: Springer-Verlag, 1987.

[2] V. A. N. Barroso and C. A. C. Belo, "A model based equalization structure for underwater communications," in *Acoustic Signal Processing for Ocean Exploration*, J. M. F. Moura and I. M. G. Lourtie, Eds. Boston: Kluwer, 1993, NATO-ASI Series.

[3] V. A. N. Barroso and J. M. F. Moura, "Adaptive beamforming as an inverse problem," in *Proc. Int. Conf. Acoust., Speech, Signal Processing, ICASSP'89* (Glasgow, Scotland), 1989.

[4] ——, "Optimal estimation and beamforming," in *Underwater Acoustic Data Processing*, Y. T. Chan, Ed. Boston: Kluwer, 1989, NATO-ASI Series.

[5] ——, "Detection performance of the l_1 beamformer in the presence of underwater burst noise," in *Proc. Int. Conf. Acoust., Speech, Signal Processing, ICASSP'90* (Albuquerque, NM), 1990.

[6] G. Bienvenu, "Passive array processing: From conventional to high resolution concepts," in *Underwater Acoustic Data Processing*, Y. T. Chan, Ed. Boston: Kluwer, 1989, NATO-ASI Series.

[7] F. Bryn, "Optimum signal processing of a 3-D array operating on gaussian signals and noise," *J. Acoust. Soc. Amer.*, vol. JASA-34, no. 3, Mar. 1962.

[8] C. I. Byrms, A. Lindquist, and T. McGregor, "Predictability and unpredictability in Kalman filtering," *IEEE Trans. Automat. Contr.*, vol. 36, no. 5, May 1991.

[9] J. Capon, "High resolution frequency-wavenumber spectrum analysis," *Proc. IEEE*, vol. 57, 1969.

[10] H. Cox, "Resolving power and sensitivity to mismatch of optimum array processors," *J. Acoust. Soc. Amer.*, vol. JASA-54, no. 3, Mar. 1973.

[11] E. Denoel and J. P. Solvay, "Linear prediction of speech with a least absolute value criterion," *IEEE Trans. Acoust., Speech, Signal Processing*, vol. ASSP-33, no. 6, Dec. 1985.

[12] U. B. Desai, *Modelling and Applications of Stochastic Processes*. Boston: Kluwer, 1989.

[13] B. Friedland, "On the properties of reduced order Kalman filters," *IEEE Trans. Automat. Contr.*, vol. 34, no. 3, Mar. 1989.

[14] A. H. Jazwinsky, *Stochastic Processes and Filtering Theory*. New York: Academic, 1970, vol. 64, *Mathematics in Science and Engineering Series*.

[15] R. E. Kalman, "A new approach to linear filtering theory and prediction problems," *J. Basic Eng. (ASME)*, vol. 83D, 1960.

[16] R. E. Kalman and R. Bucy, "New results in linear filtering and prediction," *J. Basic Eng. (ASME)*, vol. 83D, 1961.

[17] C. W. Kriel and R. Yarlagadda, "l_p estimation techniques applied to multiple emitter location," in *Proc. 4th ASSP Workshop Spectral Estimation Modeling*, 1988.

[18] K. Nagpal and C. Sims, "Linearized reduced order filtering," *IEEE Trans. Automat. Contr.*, vol. 33, no. 3, Mar. 1988.
[19] R. O. Nielsen, *Sonar Signal Processing*. New York: Artech, 1991.
[20] A. Paulraj, V. U. Reddy, and T. Kailath, "Analysis of signal cancellation due to multipath in optimum beamformers for moving arrays," *IEEE J. Oceanic Eng.*, vol. OE-12, no. 1, Jan. 1987.
[21] V. U. Reddy, A. Paulraj, and T. Kailath, "Performance analysis of the optimum beamformer in the presence of correlated sources and its behavior under spatial smoothing," *IEEE Trans. Acoust., Speech, Signal Processing*, vol. ASSP-35, July 1987.
[22] A. N. Tikhonov, "On the problems with approximately specified information," in *Ill- Posed Problems in the Natural Sciences*, A. N. Tikhonov and A. V. Goncharsky, Eds. MIR, Mathematics and Mechanics Series, 1987.
[23] H. L. Van Trees, *Detection, Estimation, and Modulation Theory, Part I*. New York: Wiley, 1968.
[24] R. Yarlagadda, J. B. Beduar, and T. L. Watt, "Fast algorithms for l_p deconvolution," *IEEE Trans. Acoust., Speech, Signal Processing*, vol. ASSP-33, no. 1, Feb. 1985.
[25] E. Yaz, "Robustness of stochastic parameter control and estimation schemes," *IEEE Trans. Automat. Contr.*, vol. 35, no. 5, May 1990.
[26] C. A. Zala, I. Barrodale, and J. S. Kennedy, "High resolution signal and noise field estimation using the l_1 (least absolute value) norm," *IEEE J. Oceanic Eng.*, vol. OE-12, no. 1, Jan. 1987.

Victor A. N. Barroso (M'89) was born in Lisbon, Portugal, on December 22, 1952. He received the E.E. degree in 1976 and the Ph.D. degree in electrical and computer engineering in 1990, both from the Instituto Superior Técnico (IST), Lisbon, Portugal.

In 1976, he joined the faculty of the Department of Electrical and Computer Engineering at IST. He was promoted to Assistant Professor in 1990 and to Associate Professor in 1993. He is also a Researcher at Centro de Análise e Processamento de Sinais (CAPS) and at the Instituto de Sistemas e Robótica (ISR), both in Lisbon, Portugal. He has taught courses in systems and signals theory, control systems, and communications. His research interests are the applications of signal processing and estimation theory, namely, in underwater acoustics and mobile communications.

Dr. Barroso is a member of several IEEE societies.

José M. F. Moura (S'71–M'75–SM'90–F'93) received the engenheiro eletrotécnico degree in 1969 from Instituto Superior Técnico (IST), Lisbon, Portugal, and the M. Sc., E.E., and the D. Sc. in electrical engineering and computer science from the Massachusetts Institute of Technology, Cambridge, MA, USA, in 1973 and 1975, respectively.

He is currently a Professor of Electrical and Computer Engineering at Carnegie Mellon University, Pittsburgh, PA, USA, which he joined in 1986. Previously, he was on the faculty of IST where he was an Assistant Professor (1975), Professor Agregado (1978), and Professor Caterdrático (1979). He has had visiting appointments at several institutions, including M.I.T. (Genrad Associate Professor of Electrical Engineering and Computer Science, 1984–1986 and associated with LIDS) and the University of Southern California (research scholar, Department of Aerospace Engineering, during the Summer through 1978–1981). His research interests lie in statistical signal processing (one and two dimensional), array processing, underwater acoustics, and multiresolution techniques. He has over 120 technical contributions, including invited ones, published in international journals and conference proceedings and is co-editor of the books *Nonlinear Stochastic Problems* (Reidel, 1993) and *Acoustic Signal Processing for Ocean Exploration* (Kluwer, 1993). He has organized and co-directed two international scientific meetings on signal processing theory and applications.

Dr. Moura was elected corresponding member of the Academy of Sciences of Portugal (Section of Sciences) in July 1992. He has been a member of the IEEE Press Board since 1991, a technical associate editor for the IEEE SIGNAL PROCESSING LETTERS, and a member of the Underwater Acoustics Technical Committee of the Signal Processing Society. He was an associate editor for The Signal Processing Transactions (Sonar and Radar) from 1988 through 1992 and a member of the technical committee of The IEEE International Symposium on Information Theory (ISIT 1993). He is affiliated with several IEEE societies, Sigma Xi, AMS, IMS, SIAM, and Ordem dos Engenheiros.